

5

Radiation Interactions in Matter

Roberta A. Bigelow

5.1 Introduction

Much of the physics of nuclei and particles is studied experimentally through the measurement of scattering and emission of various types of radiation. An understanding of how radiation interacts with matter is necessary for an understanding of how to make and interpret these measurements. There are three types of radiation which are classified in terms of their interactions with matter: charged particles, photons, and other neutral particles. NUCRAD will consider charged particles and photons.

The basic features of radiation interaction with matter that we will investigate are ranges, energy loss by the particles (dE/dx), energy distribution of scattered particles, and the random paths that particles follow in matter. Through running this simulation, you will develop an understanding of how these features depend on the interaction material, the type of radiation, and the energy of the particle. You will develop an understanding of why the concept of range must be treated differently for photons, electrons, and heavy charged particles, and how photon and electron interactions with matter contribute to the formation of a gamma ray spectrum in a sodium iodide NaI crystal.

Radiation interactions in matter are used in the diverse research areas of medical physics, radiation damage, electron microscopy, and radiation detectors. NUCRAD is a basic tool to understand the interaction of radiation with matter and it could be used as a stepping stone for more complex programs which study how radiation interacts with biological materials, how materials change when irradiated, and how detectors are constructed with specific properties. Medical physics and radiation damage studies are particularly interesting applications to significant current problems.

The simulation NUCRAD is an introduction to radiation interaction in matter, therefore, some topics have been treated in a limited way or not at all, such as Čerenkov radiation. Two books which treat these topics more extensively are

*Radiation Detection and Measurement*¹ by G. F. Knoll and *Techniques for Nuclear and Particle Physics Experiments*² by W. R. Leo. Radiation detectors are a logical subject to explore after using NUCRAD, and a good source of information is Knoll's book.¹ Textbooks which treat the topics of radiation interacting in matter and radiation detectors are listed in the references.³⁻⁹

The users of this simulation should have a background in modern physics. While a background in quantum mechanics is not a prerequisite for using NUCRAD, it is necessary for understanding many of the equations in this text.

NUCRAD is divided into two major sections: the general interaction of radiation with matter and a specific application to the detection of photons with a NaI crystal.

5.2 General Radiation and Matter

5.2.1 Assumptions and Limitations

The focus of NUCRAD is on the loss of energy and scattering of the incoming (primary) radiation. Often the interaction of these particles with matter result in additional or secondary radiation such as electrons ejected from atoms in the photoelectric effect. Calculating the interactions of secondary radiation is important in understanding where energy is deposited in a material; however, following all the secondary radiation is complicated and time-consuming. The treatment of secondary radiation is not explored in the general radiation portion of NUCRAD, but secondary radiation for the different sources is indicated in the discussion below. Since secondary calculations are not considered, some topics cannot be studied directly, such as radiation damage. Appropriate problems to explore with NUCRAD are, however, beam broadening or backscattering out from the front face of the material.

Radiation scattering into the absorber from surrounding material is an important experimental concern because it distorts the energy response of the absorber. If radiation scatters before entering the absorber or if radiation which escaped the absorber is scattered back in, the radiation enters the absorber with a degraded energy. An accurate treatment is dependent on the exact experimental setup and would be prohibitive regarding computer time, therefore radiation scattered into the absorber is not included in NUCRAD.

5.2.2 Theoretical Background

Charged Radiation

The primary interaction of charged particles with matter are inelastic collisions with the atomic electrons of the material. These interactions occur often over the path of the particles and result in energy loss by the particles and deflection of the particles from their incident direction.

The charged particles are normally considered in two separate groups, the heavy and the light charged particles, since the details of their interactions with

matter are different. Electrons and positrons form the light charged particle group and all others form the heavy charged particle group.

Heavy Charged Particle Radiation

Heavy charged particles can either excite or ionize the atoms of an absorber material. The incident particles lose little energy in a collision with an electron; the maximum energy that can be transferred in a single collision is $4Tm_e/m$, where T is the kinetic energy of the incident particle, m is its mass, and m_e is the mass of an electron. To lose a significant amount of energy the particle must undergo a large number of collisions. At any given time, the particle is interacting with many electrons, so we assume that its velocity continuously decreases until the particle is stopped. The energy loss formula for heavy charged particles is known as the Bethe-Bloch formula,^{1,3}

$$-\frac{dE}{dx} = \frac{4\pi r_e^2 m_e c^2 z^2}{\beta^2} NZ \left[\ln \frac{2m_e c^2 \gamma^2 \beta^2}{I} - \beta^2 \right], \quad (5.1)$$

where $\beta = v/c$, v and ze are the velocity and charge of the incident radiation, $\gamma = 1/\sqrt{1 - \beta^2}$, N and Z are the number density and atomic number of the absorber atoms, $r_e = e^2/m_e c^2$ (the classical electron radius), and e is the electronic charge. The parameter I represents the average excitation and ionization potential of the absorber usually included in the calculation as an experimentally determined quantity. The Bethe-Bloch formula breaks down at low energies where the particle velocity is comparable or smaller than the orbital velocity of electrons in the absorber. There are two correction factors, the density effect and the shell correction, that are needed at high and low energies, respectively.²

A monoenergetic beam of heavy charged particles will lose energy as they pass through matter until they are all stopped at approximately the same place. The number of particles scattered out of the beam is very small because individual particles are not greatly deflected in any one encounter. The minimum amount of material that will stop a beam of particles is defined as the range. Because the energy loss for individual particles is a statistical process, there is a fluctuation in the range for particles with the same initial energy. Often the mean range is used—the distance where one-half the particles have longer ranges and one-half have shorter ranges. The variation about the mean range is usually small. The range depends on the type of particle, the incident energy, and the material. At low energies where particles have velocities comparable to the velocity of the orbital electrons Eq. 5.1 breaks down.

The secondary radiation created by the heavy charged particles is made up of ionized electrons, called delta rays. Delta rays have sufficient kinetic energy to create further ions, but their range is much smaller than that of the incident particle.

Light Charged Particle Radiation

The primary energy loss mechanism at low energy for light charged particles is due to inelastic collisions with atomic electrons. The collision energy loss

formula Eq. 5.1 must be modified since the mass of the incident particles is the same as the atomic electrons and for electrons the collisions take place between identical particles. Electrons and positrons can be significantly deflected in collisions, transferring a maximum energy of $T/2$ in the collision where T is the incident particle kinetic energy, as before. Since a much larger fraction of the electron energy can be lost in a single encounter, it takes only a few collisions to lose a significant amount of energy. Energy losses due to collisions for electrons is described by the Bethe-Bloch formula,³

$$-\left(\frac{dE}{dx}\right)_c = \frac{2\pi r_e^2 m_e c^2}{\beta^2} NZ \cdot \left[\ln \frac{m_e c^2 \beta^2 T \gamma^2}{2I^2} - \ln 2 \left(\frac{2}{\gamma} - \frac{1}{\gamma^2} \right) + \frac{1}{\gamma^2} + \frac{1}{8} \left(1 - \frac{1}{\gamma} \right)^2 \right], \quad (5.2)$$

where the symbols have the same meaning as in Eq. 5.1. The equation for energy loss due to collisions for positrons differs from Eq. 5.2 in the last three terms and can be found in Leo² (p. 35).

When electrons and positrons undergo large accelerations due to electrostatic attraction to the nucleus, they emit electromagnetic radiation called *bremsstrahlung*. The energy loss is described by³

$$-\left(\frac{dE}{dx}\right)_r = 4r_e^2 Z^2 \alpha N E_0 \left[\ln \frac{2E_0}{m_e c^2} - \frac{1}{3} \right], \quad (5.3)$$

where $\alpha = 1/137$, the fine structure constant, and E_0 is the initial total energy of the electron or positron. This equation for radiative energy loss is valid when $m_e c^2 \ll E_0 \ll m_e c^2 Z^{1/3} / \alpha$. An equation for radiative energy loss when $E_0 \gg m_e c^2 Z^{1/3} / \alpha$ is given in Leo.² The total energy loss for electrons is the sum of Eqs. 5.2 and 5.3. The probability for emitting *bremsstrahlung* is inversely proportional to the square of the particle mass, so it can be ignored for heavier particles. At energies less than a few MeV this process is a relatively small factor; however, as energy increases the probability of *bremsstrahlung* increases rapidly and comes to dominate the energy loss. *Bremsstrahlung* photons form one type of secondary radiation for electrons and positrons; the paths or histories of these photons is not followed in NUCRAD.

The pathlength of an electron in a material is often much longer than the straight line penetration depth due to the many deflections along the path; therefore the range is a less definite quantity for electrons than for heavy charged particles. A method for calculating reproducible range values is extrapolating to zero the linear portion of a plot of electron transmission versus absorber thickness which has been corrected for background radiation. Very few electrons penetrate this value of absorber thickness. Empirical range-energy relationships are often used to calculate ranges in particular materials.⁴

Photon Radiation: Photoelectric Effect

The important interactions for photons in matter are the photoelectric effect, Compton scattering, and pair production. The photoelectric effect is the absorption of a gamma-ray by a bound electron which then leaves the atomic state that it

occupied. The most tightly bound electrons, the K-electrons, contribute the most to this effect. The photoelectric cross section is difficult to calculate because of the complexity of the Dirac wave functions for the atomic electrons. For various applications, empirical formulas are used instead, such as the one below for $E > 0.2\text{MeV}$:

$$\sigma_k \cong Z^5 \sum_{n=1}^4 \frac{a_n + b_n Z}{1 + c_n Z} E^{-p_n}, \quad (5.4)$$

where a_n , b_n , c_n , and p_n are parameters fitted to experiments¹⁰ and all cross sections are given in barns ($1b = 10^{-24}\text{cm}^2$). This is the cross section due to the K-shell electrons. An empirical formula is used to account for the contribution of the outer shells:¹⁰

$$\frac{\sigma_{PE}}{\sigma_k} = 1 + 0.01481(\ln Z)^2 - 0.000788(\ln Z)^3. \quad (5.5)$$

The probability for photoelectric absorption varies approximately as the fifth power of the atomic number of the medium and decreases quite rapidly as the energy of the gamma-ray photon increases, except near a resonance region (see Fig. 5.1 with $E = 0.1\text{ MeV}$). The photoelectric effect dominates at low energies. The photoelectrons which are ejected from the atoms and the accompanying *bremsstrahlung* radiation are the major types of secondary radiation in the photoelectric effect. The kinetic energy of the photoelectrons is

$$T_{e^-} = E_\gamma - E_b, \quad (5.6)$$

where E_γ is the gamma energy and E_b is the binding energy of the electron. In general the photoelectron has enough energy to produce many secondary ion pairs as it passes through matter. The energy acquired by the atom in the ejection of the photoelectron is given up later as x-ray photons when the vacated orbit is filled. These secondary electrons and x-ray photons are additional types of secondary radiation in the photoelectric effect.

Compton Scattering

In Compton scattering a gamma ray of energy E is scattered by one of the free or loosely bound electrons of the material. The scattered gamma ray energy E' as a function of the photon scattering angle θ is given below:

$$E' = E \left[1 + \frac{E}{m_e c^2} (1 - \cos \theta) \right]^{-1}. \quad (5.7)$$

The gamma ray photon is scattered off in a new direction with a lower energy. A beam of gamma rays broadens and loses energy in a succession of Compton scatterings as it passes through matter. The differential cross section for collisions between the incident photon and an electron is given in the Klein-Nishina formula,

$$\frac{d\sigma_c}{d\Omega} = \frac{r_e^2}{2} \frac{1}{[1 + x(1 - \cos \theta)]^2} \left(1 + \cos^2 \theta + \frac{x^2(1 - \cos \theta)^2}{1 + x(1 - \cos \theta)} \right), \quad (5.8)$$

where $x = E/m_e c^2$. The total cross section per electron for a Compton scattering is

$$\sigma_c = 2\pi r_e^2 \cdot \left\{ \frac{1+x}{x^2} \left[\frac{2(1+x)}{1+2x} - \frac{1}{x} \ln(1+2x) \right] + \frac{1}{2x} \ln(1+2x) - \frac{1+3x}{(1+2x)^2} \right\}. \quad (5.9)$$

The total cross section per atom is $Z\sigma_c$. The probability for Compton scattering varies approximately as the atomic number of the scattering medium and decreases as the energy of the gamma ray photon increases. Compton scattering dominates at medium energies (see Fig. 5.1). A Compton-recoil electron and the *bremsstrahlung* that it produces constitute the secondary radiation in a Compton scattering event.

Pair Production

In the presence of other matter, gamma rays of energy greater than or equal to 1.02 MeV may create positron-electron pairs. The photon vanishes and a positron and an electron are left, such that the kinetic energies of the two particles, T_{e^+} and T_{e^-} , plus their masses is equal to the incident gamma ray energy:

$$E = T_{e^+} + T_{e^-} + 2(m_e c^2). \quad (5.10)$$

The pair production cross section depends on the incident gamma ray energy, the atomic number of the material, the resulting electron and positron energies, and the amount of screening felt by the electron and positron. The cross section can be calculated analytically for certain limiting cases, but in general, the differential cross section must be integrated numerically. NUCRAD uses a look-up table for the pair production cross section. Above the threshold energy, the probability for pair production increases with the energy of the gamma ray photon and varies

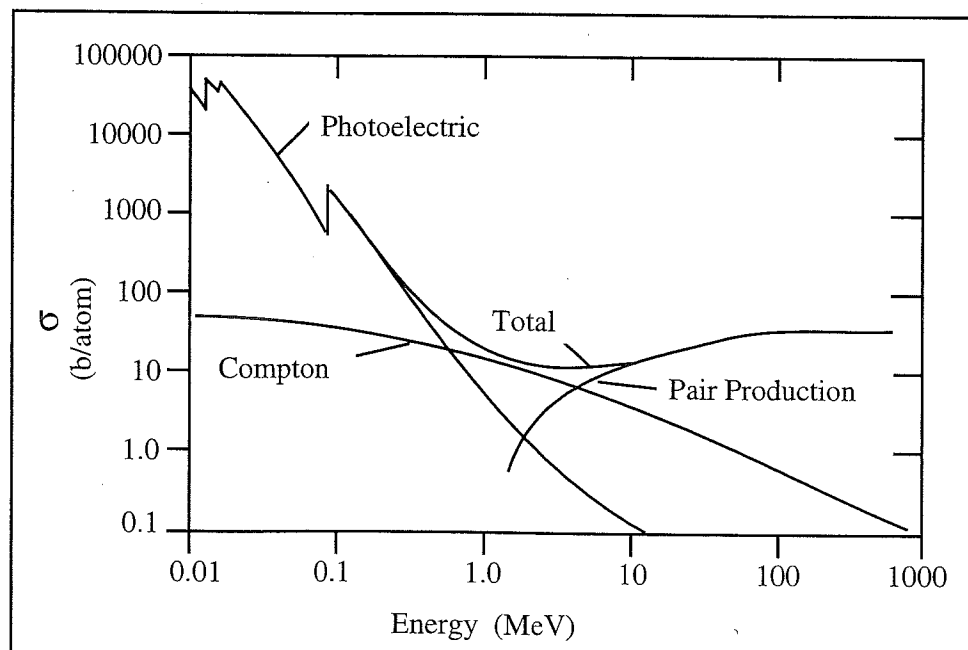


Figure 5.1: Interaction cross sections as functions of photon energy for lead.

as the square of the atomic number of the medium. The pair production process dominates at high energies.

The positron travels through the absorber and annihilates with an electron in the material when it is nearly at rest. In the annihilation two photons of 0.511 MeV are created which go off in opposite directions to each other in the laboratory system. The electron, positron, and the annihilation gamma rays form the secondary radiation in the pair production process.

The concept of range which worked so well for heavy charged particles is not appropriate for the passage of photons in matter. In two of the three photon interactions above the photon is absorbed; in the third interaction the photon loses energy and is scattered. The photons that pass straight through the material have not undergone any interactions and have their original energy. Consequently, the intensity of the incident beam I_o as it travels through matter is exponentially attenuated,

$$I(t) = I_o e^{-\mu t}, \quad (5.11)$$

where I is the intensity of the beam after traveling a distance t , and μ is the total linear attenuation coefficient. Normally μ is given in cm^{-1} so t is in cm. The total linear attenuation coefficient is the sum of the linear attenuation coefficients for each process, and these are defined in terms of their cross sections as

$$\mu_{PE} \equiv \sigma_{PE} N, \quad (5.12)$$

$$\mu_C \equiv \sigma_c Z N \quad (5.13)$$

$$\mu_{PP} \equiv \sigma_{PP} N, \quad (5.14)$$

where N is the number of atoms per cm^3 and Z is the number of electrons per atom. The quantity which can be used instead of range is the half-value layer, the thickness of absorber which attenuates the initial intensity by a factor of 2. The attenuation coefficients are often stated in terms of the mass attenuation coefficients in cm^2/g

$$\frac{\mu_{PE}}{\rho} \equiv \sigma_{PE} \frac{N_A}{M} \quad (5.15)$$

$$\frac{\mu_C}{\rho} \equiv \sigma_c Z \frac{N_A}{M} \quad (5.16)$$

$$\frac{\mu_{PP}}{\rho} \equiv \sigma_{PP} \frac{N_A}{M}, \quad (5.17)$$

where N_A is Avogadro's number and M is the atomic weight in g/mol.

5.3 Radiation Interaction in NaI

The energy response of a NaI detector to photons is determined by considering the transport of the photons and the resulting secondary radiation through the detector. Gamma radiation from a source enters the detector, moves through it, and either is absorbed or escapes from the detector. The secondary radiation that is produced also moves through the detector until it is captured or escapes. The total energy deposited by the incident photons and secondary radiations is the quantity which is calculated to determine the energy response of the detector.

5.3.1 Assumptions and Limitations

Background radiation is not considered by NUCRAD. The background radiation is due to many processes, such as source radiation which scatters into the detector from the surrounding apparatus or air, and radiation that escaped the detector and is backscattered into it. The background is dependent on the experimental set-up and, therefore, not suitable to put into a general calculation such as this. The photon interactions that are considered here are the photoelectric effect, Compton scattering, and pair production. All other interactions are assumed to be negligible in the allowed photon energy range of 0.3 to 2.5 MeV. When a photon energy drops below 0.02 MeV, the photon is considered to be absorbed and removed from the beam.

Secondary radiation is considered in this section, in the form of electrons and positrons. However, the calculations assume that the electrons and positrons lose energy where they are created and therefore none of them escape from the crystal. The distance these particles travel before stopping is small at the energies considered here and their paths are twisted, so this simplification is reasonable. As a result, the eventual positron annihilation also takes place where it was created. *Bremsstrahlung* from the electrons and positrons is ignored because it is a small effect below the maximum allowed photon energy. At higher energies there is more *bremsstrahlung* with the possibility that some of this secondary radiation escapes, thereby affecting the shape of the detector response curve.

5.3.2 Theoretical Background

Photons ionize or excite the atoms of the NaI detector as they interact. When the atoms de-excite they emit radiation in the visible or near visible region. The light hits the photosensitive surface of the photomultiplier tube, where photoelectrons are emitted and multiplied to produce an electrical pulse. The pulse is nearly proportional to the energy collected in the crystal. It is analyzed according to magnitude and recorded as a histogram of points to form the detector energy response spectrum.

If we had a perfectly absorbing ideal detector with no background radiation, we would expect to see a single spike in the histogram which would correspond to the energy of the incident monoenergetic photons. However, there are two major factors which change the shape of the energy response: (1) in a real detector some of the incident and secondary radiation escapes and (2) the statistical nature of the detector system which causes a broadening of the response spectrum. The only secondary radiations which can escape according to the assumptions made in NUCRAD are the Compton scattered photons. Since scattering angles from 0 to π are allowed we see from Eq. 5.7 that if the Compton scattered photon escapes, a continuum will result from zero energy to the so-called Compton edge (see Fig. 5.2). The energy at the Compton edge is equal to the maximum kinetic energy that can be transferred to an electron in a single Compton interaction,

$$T_{e_{max}} = E_{\gamma} \frac{2E_{\gamma}/m_e c^2}{1 + 2E_{\gamma}/m_e c^2}, \quad (5.18)$$

where $T_{e_{max}}$ is the maximum kinetic energy imparted to the electron and E_{γ} is the

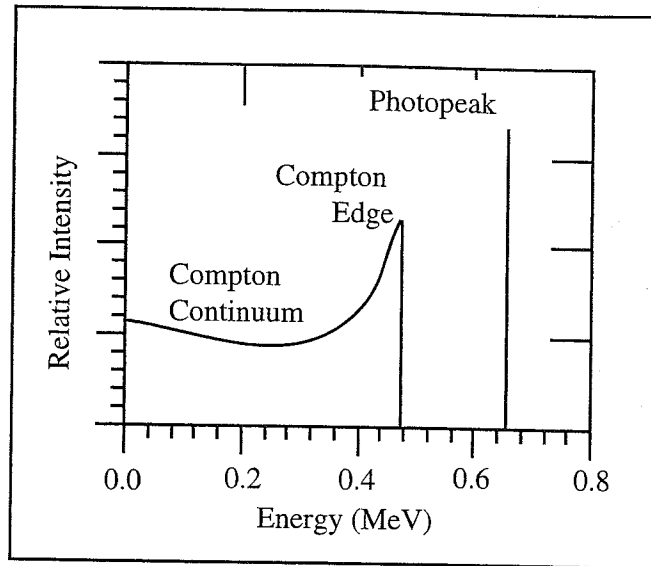


Figure 5.2: Detector energy response to 0.662 MeV photons showing the Compton continuum and photopeak before broadening.

gamma ray energy.

Both the production of photoelectrons in the photomultiplier tube and their subsequent multiplication are processes subject to random fluctuations. These processes cause a spreading of the Compton edge and the photopeak. Due to the random nature of the fluctuations, it is plausible that a Gaussian distribution would approximate the spreading, and it is given by

$$f(E, E')dE = (\pi\sigma^2)^{-1/2} \exp\left[-\frac{1}{2}(E - E')^2\sigma^{-2}\right]dE, \quad (5.19)$$

where $f(E, E')dE$ is the probability that an energy E' deposited in the detector will give a response pulse with height E in dE . The quantity σ has a dependence on E' which can be expressed empirically by the relation¹³

$$\sigma = A\sqrt{E'} + BE', \quad (5.20)$$

where A and B are constants which differ from one counter to another. The broadening effect is applied after the main calculation is finished.

5.4 Computational Approach

5.4.1 Overview

The experimental arrangement for the general radiation calculation is a narrow parallel beam that impacts a uniform slab of material at the center of the front face. Each source particle enters the material normal to the front face at the Cartesian coordinates (0,0,0). The experimental arrangement for photons interacting with a

cylindrical NaI detector consists of a isotropic point source on the detector axis. The z -axis coincides with the detector axis and the origin is at the detector face nearest the source. The point of impact and direction of the source particles are randomly determined.

NUCRAD uses Monte Carlo methods to simulate radiation interacting in materials. Details of using the Monte Carlo technique to study radiation transport in matter are described in several sources.¹¹⁻¹⁷ In the general radiation calculations individual histories are considered for the source particles. However, the main calculation of the response function of a NaI detector is done by weighting each source particle with survival probabilities and then using statistical estimation to obtain the response function. For the annihilation radiation, individual histories are calculated and folded into the statistical estimation.

5.4.2 Program Procedures—General Radiation in Matter

The objective is to calculate where collisions take place in the material, determine the nature of the collision, and determine the immediate fate of the particle after the collision. Once the choices of radiation, initial energy, and material have been made, the path history of a source particle is calculated in one of the procedures **pathCalcHeavy**, **pathCalcElectron**, or **pathCalcPhoton**. For each step of the path a pathlength, an energy loss, a change in direction, and a spacial displacement must be calculated. The pathlength is calculated in either **NextCollision** or **NextCollisionHeavy**. The **MidParamHeavy**, **MidParamElectron**, and **MidParamPhoton** procedures calculate the scattering angle and the resultant energy of the deflected particle based on the continuous-slowing-down approximation. **DirectionAfterScatt** calculates the new direction cosines to be used in **NextCollision** or **NextCollisionHeavy** in the calculation of the next collision position.

The **pathCalc...** procedures call either **NextCollision** or **NextCollisionHeavy** to decide whether the particle has escaped, undergone a collision, or moves along its line of flight without incident. First these two procedures must calculate the pathlength that the radiation particle travels between collisions. In **NextCollision-Heavy** a pathlength for an alpha particle or muon is calculated such that, on average, the energy of the particle is reduced by a constant amount, k , per path step.

$$\text{pathlength} = \frac{E(1 - k)}{dE/dx}. \quad (5.21)$$

The reduction factor is chosen so that in the absence of energy loss fluctuations the particle will lose half its energy in an integral number of steps, m , from $k = 2^{-1/m}$. The pathlength in **NextCollision** calculated from the mean free path which is computed in **CalculateLambda** from the cross section. **CalculateLambda** calls **CalcSigElectron** for electrons and **CalcSigCompton**, **CalcSigPhotoelectric**, and **CalcSigPair** for photons to compute cross sections. The pathlength traveled by the particle is then randomly selected from an exponential distribution according to the formula

$$\text{pathlength} = -\lambda \ln(r), \quad (5.22)$$

where λ is $(N\sigma_{total})^{-1}$ and r is a random number chosen from the interval $[0, 1]$.

To determine whether or not the particle has escaped, the Cartesian coordinates of the collision point are calculated from the direction cosines of the last collision point and the pathlength. If the particle escapes out the front face or back face of the material, either the reflected or transmitted counter is incremented and a fresh particle is introduced. **PathCalc...** then calls the procedure **PlotPath** to draw a line from the last collision point to the present collision point in the path display window.

Next, **PathCalc...** calls one of the procedures **MidParamHeavy**, **MidParamElectron**, or **MidParamPhoton** to calculate the laboratory angle of deflection from the line of flight and the energy of the particle after deflection. At this point, a check of the energy is made to determine whether the particle has been absorbed. The determination is based on the particle energy dropping below a cutoff energy; 0.01 MeV for photons, 0.005 MeV for electrons, 0.50 MeV for alphas, and 0.08 for muons. In the event of an absorption, the absorbed counter is incremented and a fresh particle is introduced. If the particle is to be followed further, the new direction cosines are calculated in a purely geometric procedure, **DirectionAfterScatt**, and the next collision point is calculated in **NextCollision** or **NextCollisionHeavy**. This set of procedures is followed until all the source particles have been considered.

After the path histories of all the particles have been calculated additional calculations are done for the source particles. For photons, the cross section versus energy is calculated in **PhotonSigma** and the first scattering angle for each particle which undergoes a Compton event is calculated in the main photon procedure **PathCalcPhoton**. For charged particles the energy loss versus energy is calculated either **dEdxCalcElectron** or **dEdxCalcHeavy** and the energy distribution of the transmitted particles is calculated in **ETransmit**. If the range or the attenuation calculation is chosen in the experimental input screen, the path histories for the particles are calculated for 11 different absorber thicknesses, and a graph of transmission versus absorber thickness is plotted.

5.4.3 Program Procedures—Radiation Interaction With NaI

To calculate the energy response of a NaI detector, the total energy deposited in the detector by the photon interactions, photoelectric effect, Compton scattering, and pair production must be known. The process used to make this calculation was to begin with a isotropic point source and follow the interactions of N source photons with NaI. A source particle was assigned a weight of N^{-1} and the impact point and direction were calculated. The first collision point was found based on the mean free path and the cross sections for the three photon interactions. At this collision the particle was assumed to undergo a photoelectric event, a pair production event if the energy exceeded threshold, and a Compton scattering event. As each type of interaction was considered, the weight of the particle was adjusted to account for the probability of undergoing the interaction. In the case of a pair production event, the individual histories of the annihilation photons were calculated. In the case of Compton scattering, the source particle was not allowed to escape the detector; however, the weight was adjusted to take into account the probability of surviving. The process of selecting collision points and considering the various interactions was repeated until either the photon energy was reduced below 0.01 MeV or its

tes
on
ice
l a
aw
lay
m-
on
nt,
ed.
gy;
for
d a
ec-
att,
vy.
id-
nal
sus
cle
ure
ted
the
ion
the
of
the
and
s to
ons
and
ean
sion
vent
e of
for
ent,
e of
:tor;
ing.
ions
r its

weight was below $0.001 N^{-1}$. A fresh source photon was then introduced until photons had been considered.

The procedure **NaICalc** calls **InitialNaIvalues** to calculate the initial position and direction of the source particle in the detector. The direction of the source photon was defined by the direction cosines for the x -, y -, and z -axes or α , β , and γ ; respectively. The direction cosine, γ , is chosen randomly by

$$\gamma = (1 - \gamma_0) \frac{i - r}{N} + \gamma_0, \quad (5.23)$$

where γ_0 is the minimum cosine with respect to the z -axis subtended by the detector and i is the current photon number. The azimuthal angle of the source is assumed to be uniformly distributed so that we can assume, without loss of generality, that all the particles impact on the x -axis. The impact point is $x = D(1 - \gamma^2)^{1/2}/\gamma$, $y = 0$, and $z = 0$.

The distance to a collision point was selected from a truncated exponential distribution and given by

$$distance = -\lambda \ln\{1 - r[1 - \exp(-x_e/\lambda)]\}, \quad (5.24)$$

where λ is the mean free path, r is a random number chosen on the interval $[0, 1]$, and x_e is the distance to the edge of the detector calculated in **CalcDistanceXtal**. This forced the collision to be inside the detector, but to adjust for this, a weight was attached to the sample photon which was equivalent to the probability that it remained in the detector, or $1 - \exp[-x_e/\lambda]$. To calculate the mean free path of a source photon in NaI and the probability for a particular photon interaction to occur, **NaICalc** calls **CalcSigma** to read the photoelectric, Compton scattering, and pair production cross sections from tables and then calculate the total linear attenuation coefficient, μ . At each collision the radiation is assumed to undergo a photoelectric event in **PhotoElectric** and then a pair production event in **PairProduction** if the energy is above threshold.

In the case of the photoelectric event, all the energy of the electron is assumed to be deposited in the detector, because none of the *bremsstrahlung* radiation is allowed to escape. The weight of the source photon was then multiplied by the probability of having a photoelectric event, μ_{PE}/μ , and the product was added into the pulse-height interval corresponding to the energy deposited. The energy deposited in this case is the source energy minus the energy lost by the escape of secondary radiation from all previous Compton scattering events of the source photon.

In the case of the pair production event, the kinetic energies of the electron and positron are assumed to be deposited in the detector. However, when the positron is annihilated one or both of the annihilation photons may escape or a portion of the annihilation radiation may escape. The weight of the source photon was multiplied by the probability of having a pair production event, μ_{PP}/μ , and the product was added into the pulse height interval corresponding to the energy deposited. The energy deposited in this case is the source energy minus the energy lost by the escape of secondary radiation from all previous Compton scattering events of the source photon, minus the energy lost by the escape of secondary radiations produced in the pair production event.

Next, the photon was allowed to experience a Compton scattering event, and its weight was adjusted by the factor, μ_C/μ , which is the probability of scattering. The energy and direction of the photon after scattering were calculated in **CalcComptonScatt** by a method devised by Kahn in 1954 from the Compton scattering cross section. After each Compton scattering, the current weight of the photon was adjusted by the probability of escape, $\exp[-\mu x_e]$ and added into the pulse-height interval, which included the total energy deposited up to that particular collision. In this case the energy deposited is the source energy minus the current energy of the source photon minus all energy lost from the detector by the escape of secondary photons produced in all the Compton events.

The Procedure **ResponseSpectrum** was called each time an event is added to the spectrum and at the end the response spectrum was broadened with a Gaussian distribution in the Procedure **CalcBroadenSpect**.

5.5 Exercises

5.1 Attenuation of ^{22}Na Gammas

Make a preliminary design of a container to hold a ^{22}Na ($E_\gamma = 1.27$ MeV) calibration source. Choose a reasonable material from the NUCRAD selection and estimate the wall thickness to reduce the radiation intensity by a factor of 100. What is the necessary wall thickness to reduce the intensity by a factor of 1000? Explain your reasoning.

5.2 Selective Attenuation

In your experiment you are interested in making measurements with 0.45 MeV gammas, however, the source emits gamma rays of 0.15 MeV and 0.45 MeV. The 0.15 MeV gammas are 10 times more intense than the 0.45 MeV gammas, and you want to reduce their intensity without affecting the 0.45 MeV gammas. Choose a material that will reduce the 0.15 MeV gamma intensity by a factor of 100 but has as small an affect on the 0.45 MeV gammas as possible. How much is the 0.45 MeV gamma intensity reduced?

5.3 Photoelectric Absorption

What is the probability that a 0.662 MeV gamma ray from ^{137}Cs undergoes photoelectric absorption in 1 cm of lead? in 1 cm of silicon? in 1 cm of aluminum? What is the mean free path of a 0.662 MeV gamma ray in lead, silicon, and aluminum?

5.4 Gammas in NaI

You are interested in measuring the 0.847 MeV gamma rays from ^{56}Co with a NaI detector; however, the higher energy gamma rays are unwanted background, especially the one at 1.238 MeV. Find the optimum thickness of the NaI crystal.

5.5 Electrons in Aluminum

You want to eliminate background radiation of 0.1 MeV electrons in an experiment. How thick must the aluminum absorber be to stop the

electrons? How much affect does this absorber have on the 0.1 MeV gammas that you are interested in measuring?

5.6 Electron Backscattering

Since electrons go through many scatterings over their path, there is a possibility for an electron to escape from the absorber through the face that it entered. This phenomenon of backscattered electrons is important to study in connection with choosing materials for electron detectors and in other areas such as electron microscopy. Make a study of electron backscattering from aluminum and lead. First, discuss how the backscattering changes as a function of absorber thickness for a particular energy in each material and why it changes in that way. Next, consider backscattering as a function of incident electron energy. Discuss trends for a particular material and contrasts between materials. Backscattering as a function of absorber thickness is plotted in the electron range calculation.

5.7 Reducing Energy of an Electron Beam

You need 0.80 MeV electrons for a measurement, but the only source you have is a narrow beam of 1.0 MeV electrons. What absorber material and thickness will you use to reduce the energy of the 1.0 MeV electrons? Explain reasons for your choice.

5.8 Transmitted Energy Profile for Electrons

- Calculate the stopping power for 0.05 MeV electrons in aluminum, either using Eq. 5.2 or a graph of the stopping power. Estimate the energy lost by electrons passing through 50 μm of aluminum and compare with results from running NUCRAD. Repeat the calculations for incident electron energies of 0.1 and 0.5 MeV. Discuss the differences in the energy spectra of the transmitted electrons for the three different energies.
- Choose one of the energies above and explore the dependence of the transmitted electron energy spectrum on absorber thickness. Increase the thickness from 50 μm by a factor of at least 2. Discuss changes in the shape of the spectrum, the probable transmitted energy, and the average transmitted energy.
- Choose at least two other absorber materials and explore the dependence of the transmitted electron energy spectrum on material.

5.9 Electrons in a NaI Crystal

The NaI detector simulation assumes that no secondary electrons escape from the crystal, thereby depositing all their energy in the crystal. Find the range of a 0.663 MeV electron in NaI and calculate the percentage of the total volume of a 7.62×7.62 cm cylindrical crystal that lies near enough to the surface so that electron escape is possible. Repeat the calculation for a 1.28 MeV and 1.78 MeV electron.

5.10 Particle Identification for Nonrelativistic Charged Particles

Two semiconductor detectors, a thin transmission detector placed in front of a thick full absorption detector, are often used to identify charged particles. The energy loss of a particle passing through a transmission or ΔE detector is measured in coincidence with a signal from the full absorption

or E detector. Using Eq. 5.1, argue that the product $E(dE/dx)$ is mainly dependent on the mass and charge of the incident radiation. Verify this relationship using alphas passing through 10 μm of silicon with various energies between 3 and 5 MeV.

5.11 Stopping Time

The time to slow down and stop a charged particle in a material can be estimated from its range, R , and average velocity, $\langle v \rangle$ (see Knoll,¹ pp. 38-39),

$$t = \frac{R}{\langle v \rangle}.$$

A charged particle usually loses energy faster near the end of its path, so the average velocity is assumed to be about $0.6v$, where v is calculated from the initial energy. Using this relationship, estimate the time required for a 2 MeV alpha particle to slow down and stop in silicon and in air.

5.12 dE/dx

A beam of 0.1 μA alphas with kinetic energy of 6 MeV passes through a 4 μm thick silicon detector. Compute the maximum energy deposited per second in the silicon.

5.13 Scaling Laws

When range or energy loss data for a particular particle or absorber material is not available, semi-empirical formulas, usually based on Eq. 5.1, are used. In addition, an assumption is made that the stopping power per atom for compounds is additive³:

$$\frac{1}{N_c} \left(\frac{dE}{dx} \right)_c = \sum_i W_i \frac{1}{N_i} \left(\frac{dE}{dx} \right)_i, \quad (5.25)$$

where N is the atomic density, W_i is the atom fraction of the i th element in the compound, and c refers to the compound. The scaling law for ranges is commonly called the *Bragg–Kleeman rule*:

$$\frac{R_1}{R_2} \cong \frac{\rho_2 \sqrt{A_1}}{\rho_1 \sqrt{A_2}}, \quad (5.26)$$

where R is the range, ρ is the density, and A is the atomic weight. Estimate the range of 5 MeV alpha particles in silicon, then using Eq. 5.26 calculate the range of 5 MeV protons in silicon.

5.14 Compton Edges

Derive Eq. 5.18, the maximum energy given to an electron in Compton scattering. Use that formula to verify the position of the Compton edges at the incident gamma energies of 0.511, 1.28, and 1.78 MeV using the NaI detector simulation. Considering the shape of the Compton edge, is it useful for energy calibrations?

5.15 Gamma Interactions in NaI

- Estimate the mean free path of a 1.5 MeV gamma ray incident on a NaI detector and determine the dominant interaction process.

inly
this
ous

can
oll,¹

t, so
ated
ired
r.

gh a
l per

erial
are
atom

5.25)

ment
nges

5.26)

mate
ulate

ipton
edges
g the
, is it

1 NaI

b. A gamma ray can undergo multiple Compton scattering events before escaping the crystal, thereby adding a count in the pulse height spectrum between the full-energy peak and the Compton edge. What is the maximum energy that the 1.5 MeV gamma ray can deposit in two Compton scatterings before escaping from the crystal?

c. In two general Compton scatterings does the energy deposited change if the sequence of the scattering angles is reversed? Consider, for example, the scattering angles 10° and 45° .

5.16 Intrinsic Efficiency

Examine the intrinsic efficiency for the 7.62×7.62 cm detector for eight different source-detector distances between 2 and 50 cm for a gamma ray source of 0.662 MeV. Plot the efficiency as a function of distance and give some reasons for the shape of the curve. (See Marion and Young¹⁸ for graphs of intrinsic efficiency as a function of detector size.)

5.17 Response Spectrum Shape and Dependence on Energy

Consider the response spectrum for 1.78 MeV gamma rays 10 cm from the detector. Describe the processes which contributed to the various features in the spectrum. Consider spectra for 0.662 MeV and 2.5 MeV gammas. Describe the differences in these spectra compared to the first and explain why these differences occur.

5.5.1 Possible Program Modifications

• Other Materials and Sources

The first obvious extensions are to include other materials and heavy charged particle sources (e.g., protons and deuterons). This should be a straightforward extension and therefore will be a good way to become comfortable with NUC-RAD.

• Challenging Sources

Three additional sources which are more challenging than a proton or a deuteron are the positron, the pion, and heavy fission fragments. The positron is difficult because one must take annihilation into account. This has some interesting applications in detectors and beta-plus decay studies. The pion is difficult because of nuclear interactions and heavy fission fragments are difficult because nuclear elastic scattering becomes a significant mode of energy transfer.

• Radiation Interaction With Biological Material

An application out of many possible ones explores the interaction of radiation in biological material. The two major topics here are medical physics uses and radiation exposure. Under the medical physics topic the simulation could consider beams of neutrons and pions to treat specific areas of the body. Under the topic of radiation exposure, bulk radiation damage in humans and radiation damage for specific areas (e.g., skin and tissue or organs) can be considered. While there is overlap between these topics, the emphasis is very different. This extension would lead to an understanding of how various types of radiation affect different parts of the body and to a more intuitive feel for the radiation units of rem and rad.

- **Radiation Damage**

Possible applications of radiation in matter that can be simulated are radiation damage in shielding and shielding design. A major design consideration for any radiation containment vessel is the damage sustained due to radiation and therefore how to minimize this damage through an appropriate choice of materials. In a shield design feature, several materials could be layered together to maximize shielding, e.g., paraffin to moderate neutrons, boron to slow and capture neutrons, and lead to slow and capture more neutrons. The combination of the materials acts as a better shield than any one of the materials alone.

5.6 *Details of the Program*

5.6.1 Running the Program

This section describes the menu options found in NUCRAD.

- **File**

- **About CUPS**
- **About the Program**
- **Configuration**
- **Exit**

- **Radiation** This menu provides for initial experimental conditions to be chosen: radiation source, beam energy, material, slab thickness, and the number of source particles to be considered.

- **Alpha:** The default values for the alpha particle are a beam energy of 10 MeV, a material of aluminum, a slab thickness of 0.04 cm, and 200 particles. The beam energy is limited to the range 0.5 to 100 MeV.
- **Muon:** The default values for the muon are a beam energy of 5 MeV, a material of aluminum, a slab thickness of 0.08 cm, and 200 particles. The beam energy is limited to the range 0.5 to 1000 MeV.
- **Electron:** The default values for the electron are a beam energy of 50 keV, a material of aluminum, a slab thickness of 5 μ m, and 150 particles. The beam energy is limited to the range 0.02 to 0.4 MeV.
- **Photon:** The default values for the photon are a beam energy of 0.662 MeV, a material of aluminum, a slab thickness of 2 cm, and 500 particles. The beam energy is limited to the range 0.3 to 100 MeV.

- **NaI**

- **Photons in NaI:** Choose values for the detector-source distance, the energy of the source photon, and the number of source photons to consider. After these values are entered, NUCRAD calculates the NaI response function and plots a histogram of the ideal spectrum and one of the Gaussian broadened spectrum where the maximum is normalized to 1. The default source energy is 0.662 MeV. The source energy is limited to the range 0.3 to 2.5 MeV.

References

1. Knoll, G.F. *Radiation Detection and Measurement*, 2 ed. New York: John Wiley & Sons, 1989.
2. Leo, W.R. *Techniques for Nuclear and Particle Physics Experiments*. New York: Springer-Verlag, 1987.
3. Krane, K.S. *Introductory Nuclear Physics*. New York: John Wiley & Sons, 1987.
4. Evans, R.E. *The Atomic Nucleus*. New York: McGraw-Hill, 1982.
5. Enge, H.A. *Introduction to Nuclear Physics*. Reading, MA: Addison-Wesley, 1966.
6. Frauenfelder, H., Henley, E.M. *Subatomic Physics*. Englewood Cliffs, NJ: Prentice-Hall, 1991.
7. Griffiths, D.J. *Introduction to Elementary Particles*. New York: Harper & Row, 1987.
8. Segre, E. *Nuclei and Particles*, 2 ed. Reading, MA: Benjamin/Cummings, 1977.
9. Williams, W.S.C. *Nuclear and Particle Physics*. London/New York: Oxford Univ. Press, 1991.
10. Hubbell, J.H. Photon cross sections, attenuation coefficients, and energy absorption coefficients from 10 keV to 100 GeV. *National Standard Reference Data System*, NSRDS-NBS 29, 1969.
11. Cashwell, E.D., Everett, C.J. *A Practical Manual on the Monte Carlo Method*. London: Pergamon Press, 1959.
12. Williamson, W., Duncan, G.C. Monte Carlo simulation of nonrelativistic electron scattering. *American Journal of Physics*, **54**:262-267, 1986.
13. Zerby, C.D. A Monte Carlo calculation of the response of gamma-ray scintillation counters. *Methods in Computational Physics I*, New York: Academic p. 89-134 (1963).
14. Berger, M.J. Monte Carlo Calculation of the Penetration and Diffusion of Fast Charged Particles, *Methods in Computational Physics I*. pp. 135-215, New York: Academic, 1963.
15. Seltzer, S.M., Berger, M.J. Transmission and reflection of electrons by foils. *Nuclear Instruments and Methods* **119**:157-179, 1974.

16. Goldstein, J.I., Newbury, D.E., Echlin, R., Joy, D.C., Fiori, C., Lifshin, E. *Scanning Electron Microscopy and X-Ray Microanalysis*. New York: Plenum Press, 1981.
17. Koonin, S.E. *Computational Physics*. Reading, MA: Addison-Wesley, 1986.
18. Marion, J.B., Young, F.C. *Nuclear Reaction Analysis Graphs and Tables*. Amsterdam: North-Holland Publishing Co., 1968.